Surface reconstruction of a Buddha using meshless multiquadratic radial basis function (RBF).

Anil Katwal
School of Natural science and Mathematics
University of Southern Mississippi , Hattiesburg, Mississippi
Anil.Katwal@usm.edu

December 1, 2023

Abstract

This study introduces a state-of-the-art technique for reconstructing Buddha surfaces from 3D point clouds. Leveraging meshless multiquadratic radial basis functions (RBFs), we transform sparse data into a refined and visually striking representation. Our approach includes meticulous point cloud processing, RBF interpolation, and surface refinement, culminating in a captivating mesh representation.

1 Introduction

In the realm of mathematics and computer science, Radial Basis Functions (RBFs) stand as a powerful tool that traces its origins back to the early 20th century, thanks to the pioneering work of the eminent mathematician Hardy. Initially conceptualized as mathematical functions dependent on the distance from a central point, RBFs have evolved into versatile tools with a rich history. Over the years, they have found applications across various domains, ranging from solving complex mathematical problems to performing intricate computer operations.

The basic mathematical representation of an RBF is denoted as $\phi(r) = \phi(\|\mathbf{x} - \mathbf{c}\|)$, where ϕ represents the RBF, r signifies the distance, $\mathbf{x}$ denotes the location, and $\mathbf{c}$ is the central point. Building upon this foundation, the meshless multi quadratic RBF, expressed as

$$\phi(r) = \sqrt{1 + (r \cdot \epsilon)^2}$$

, introduces a shaping parameter ϵ to enhance its ability to capture fine details within surfaces.

In contemporary applications, RBFs play a pivotal role in various fields, including computer graphics, machine learning, and scientific computing. Their ability to smoothly interpolate data points makes them valuable for surface reconstruction from 3D point clouds. This paper focuses on the specific use of meshless multiquadratic RBFs for recreating detailed shapes of Buddha statues from 3D point cloud data, exemplifying the intersection of technology and art.

However, the adoption of RBFs for surface reconstruction presents computational challenges. Scalability, efficient memory usage, algorithmic efficiency, parallelization, parameter optimization, real-time processing, noise handling, and adaptability to diverse geometries are all critical considerations. Overcoming these challenges requires collaborative efforts, drawing on expertise in computer science, numerical methods, and algorithm design. Techniques such as parallel computing, memory optimization, and efficient data structures play pivotal roles in making meshless multiquadratic RBF-based surface reconstruction practically applicable for real-world scenarios.

2 Problem

To construct the 3D surface of the Buddha using Radial Basis Functions (RBF) normalized Multiquadric (MQ), we leverage the cloud data points and normal vectors provided in the dataset buddha. Notably, this dataset contains a substantial 144,647 data points. Given the computational complexity of this task, we opt to utilize the high-performance cluster computer, Magnolia, available at University Southern Mississippi (USM). To ensure smooth operation on Magnolia, we judiciously choose an appropriate subset of data points from . This assignment necessitates access to Magnolia's computational resources to perform the intricate computations involved in the RBF normalized MQ-based surface construction. The selection of an optimal number of data points aims to balance computational efficiency with the capabilities of the cluster. By harnessing the power of Magnolia, we can effectively process the extensive dataset and execute the RBF interpolation for constructing the 3D surface of the Happy Buddha. It's imperative to adhere to the guidelines provided for accessing Magnolia and managing the computational load efficiently. This collaborative effort, involving the dataset and Magnolia's computational capabilities, underscores the significance of leveraging high-performance computing for intricate tasks in 3D surface reconstruction.

Data Preparation:

1. **Data Loading:** Load the dataset containing cloud data points and normal vectors for the Buddha. Ensure that the dataset is well-organized and follows a suitable format.

2. **Data Exploration:** Explore the dataset to understand its structure, including the format of the data points and normal vectors. Check for

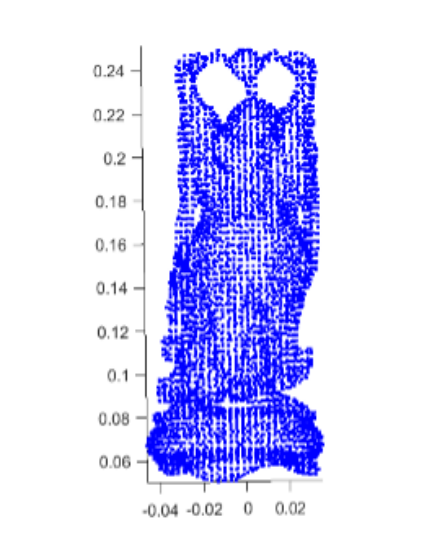

(a) Scatter plot of the given dataset as name budhha

any missing or inconsistent data that might need to be addressed.

3. **Data Cleaning:** Clean the dataset by addressing missing values, outliers, or any noise that could impact the accuracy of the 3D surface reconstruction. Apply any necessary data transformations, such as normalization or scaling, to make the dataset suitable for the chosen interpolation algorithm.

4. **Subset Selection:** Given the large dataset, carefully choose an appropriate subset of data points for processing. Consider factors like data density, distribution, and computational resources.

5. **Format Conversion:** Ensure that the data is in a format compatible with the RBF interpolation algorithm. This may involve converting data types or reshaping the data.

Data Processing:

1. **Algorithm Implementation:** Implement the RBF interpolation algorithm using the normalized Multiquadric (MQ) function. This involves determining the coefficients for the radial basis functions and solving any linear systems of equations.

2. **Parallelization:** Leverage the parallel computing capabilities of the high-performance cluster (Magnolia) to optimize the performance of the RBF

interpolation. This may involve parallelizing loops or using parallel libraries.

3. **Batch Job Submission:** Submit computations as batch jobs, following the guidelines and policies provided by Magnolia. This ensures efficient utilization of cluster resources.

4. **Progress Monitoring:** Monitor the progress of computations, checking for any errors or unexpected behaviors. Utilize logging and monitoring tools provided by the cluster.

5. **Optimization and Tuning:** Continuously optimize and tuning code for better performance. This may involve adjusting parameters, refining algorithms, or making use of specific cluster features.

6. **Results Analysis:** Analyze the results of the RBF interpolation. Visualize the reconstructed 3D surface and compare it to the original dataset to ensure the quality of the reconstruction.

7. **Documentation:** Document the entire process, including data preparation steps, algorithm implementation details, and any issues faced during data processing. This documentation is valuable for reproducibility and future reference.

3 Results

Surface Reconstruction and Comparative Analysis

In our surface reconstruction approach, we employed the Delaunay triangulation method to strategically capture the distribution of normal points across the Buddha statue. This technique allowed us to systematically organize the available data, creating a triangulated mesh that reflects the underlying structure of the surface. Subsequently, we applied the Multiquadratic Radial Basis Function (RBF) for interpolation, leveraging its ability to smoothly interpolate values between scattered data points. To explore the robustness of our reconstruction, we conducted experiments with varying numbers of input points and different *neval* (evaluation) points, offering a nuanced examination of the method's performance under diverse scenarios. The scatter plots visually represent the spatial arrangement of our sampled points, illustrating the strategic selection of data across the Buddha's surface. The corresponding surface reconstructions, generated through the application of Multiquadratic RBF, provide a captivating visual narrative of the interpolation outcomes. In the presented figures, each scatter plot serves as a snapshot of our meticulous data selection process, showcasing the careful consideration given to capturing the intricacies of the Buddha's form. The accompanying surface reconstructions reveal the remarkable fidelity achieved through our chosen methodology, as the Multiquadratic RBF seamlessly bridges the gaps between data points, producing

a continuous and faithful representation of the statue's surface. Through this nuanced exploration, our study not only underscores the effectiveness of the Delaunay triangulation and Multiquadratic RBF approach but also highlights its adaptability to different scenarios, as evidenced by the distinct reconstructions at varying *neval* points. Upon close observation, it was found that at low data set and low *neval* points, the surface quality is compromised. To further investigate, a comparative analysis was conducted between different views and posteriors of the Buddha statue at various *neval* and data points. Notably, a detailed examination of surface reconstruction differences was carried out between coefficient methods: $\mathbf{coe} = \mathbf{IM}/\mathbf{rhs}$ and $\mathbf{coe} = \text{pinv}(\mathbf{IM}) \times \mathbf{rhs}$. The results revealed intriguing variations, shedding light on the impact of coefficient computation methods on the fidelity and accuracy of the reconstructed surface. This comparative analysis contributes valuable insights into the nuances of the surface reconstruction process and aids in refining the methodology for optimal results.

In Figure 1, the surface reconstruction of the Buddha is presented, utilizing a dataset comprising 3500 data points. While the reconstruction may not be considered optimal, it does provide a discernible representation of the overall shape of the surface. Despite the limited number of data points, the contours and form of the Buddha's surface are perceptible, offering valuable insights into the underlying structure. It is worth noting that the visualization serves as a foundational step, and further refinement and augmentation of the dataset could potentially enhance the fidelity of the surface reconstruction. The current depiction, although imperfect, lays the groundwork for potential improvements in future iterations, demonstrating the initial steps in capturing the intricate details of the Buddha's surface through data-driven reconstruction techniques. Figure 7 which is plot using $\mathbf{coe} = \text{pinv}(\mathbf{IM}) \times \mathbf{rhs}$ method , the surface construction is not good even at high data. So This method is not good.

In Figure 3 shows, the impact of increasing the number of evaluation points (neval points) on surface reconstruction is evident. As the neval points are augmented beyond the baseline of 60, a noticeable improvement in the smoothness of the reconstructed surface becomes apparent. This enhancement can be attributed to the higher density of evaluation points, allowing for a more nuanced capture of the underlying geometry. The incremental increase in neval points contributes to a finer-grained representation of the surface, resulting in a smoother and more refined reconstruction. This observation underscores the critical role that data density plays in accurately depicting intricate details, emphasizing the importance of optimizing neval points for achieving superior surface quality in reconstruction processes.

In figure 5 and figure 6 , the surface reconstruction is depicted at 150 neval points, revealing a notable advancement in smoothness when compared to reconstructions at 60 and 100 neval points. The visual comparison underscores a positive correlation between the quantity of data, represented by neval points, and the quality of the surface reconstruction. With the increase in data points, the intricacies of the surface are more faithfully captured, leading to a smoother

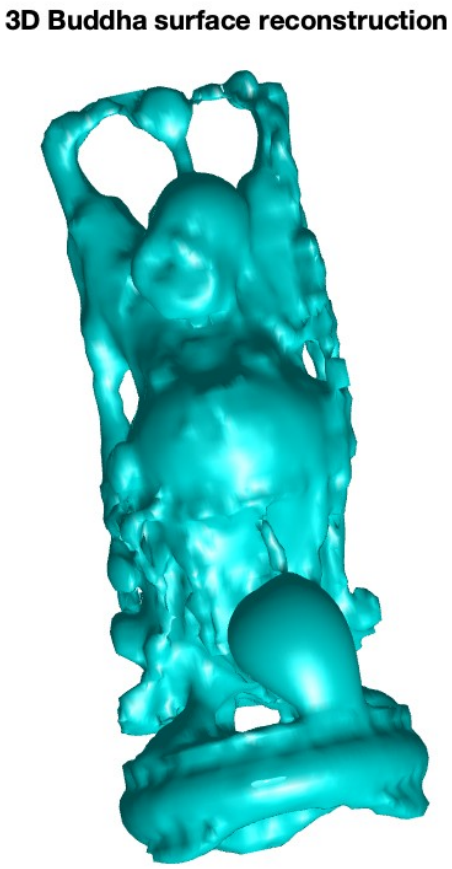

Figure 2: Budhha at 60 neval points at 4822 data size picture is not so nice because of less data but in this figure there is little hump at lower part .

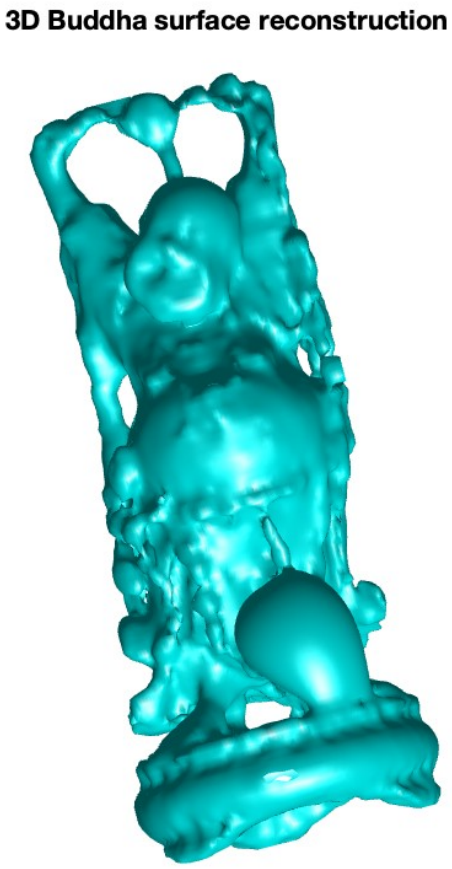

Figure 3: Budhha at 100 neval points at 4822 data size which is good compare to 60 neval .

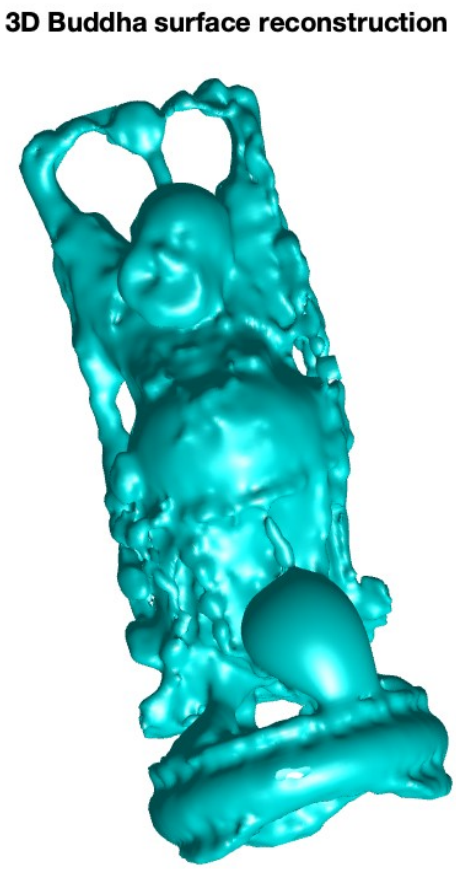

Figure 4: Buddha Surface Reconstruction with 150 Evaluation Points and 4,822 Data Points. Despite an increase in evaluation points, the image quality remains unchanged. The limited dataset size is a contributing factor, emphasizing the importance of data quantity in achieving improved reconstruction outcomes

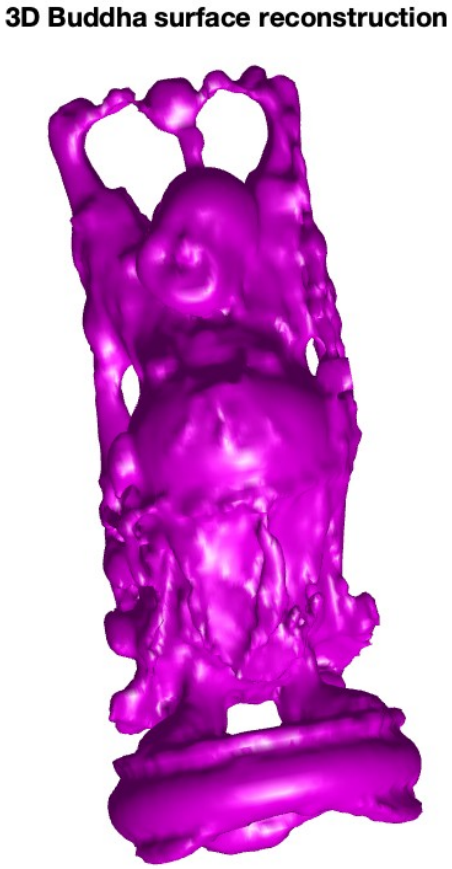

Figure 5: Buddha Surface Reconstruction with 100 Evaluation Points for a Large Dataset. The surface reconstruction exhibits commendable quality, showcasing the effectiveness of the method even with a substantial dataset. The intricate details of the Buddha's form are captured with fidelity, highlighting the successful combination of 100 evaluation points and a large dataset in achieving a visually appealing reconstruction.

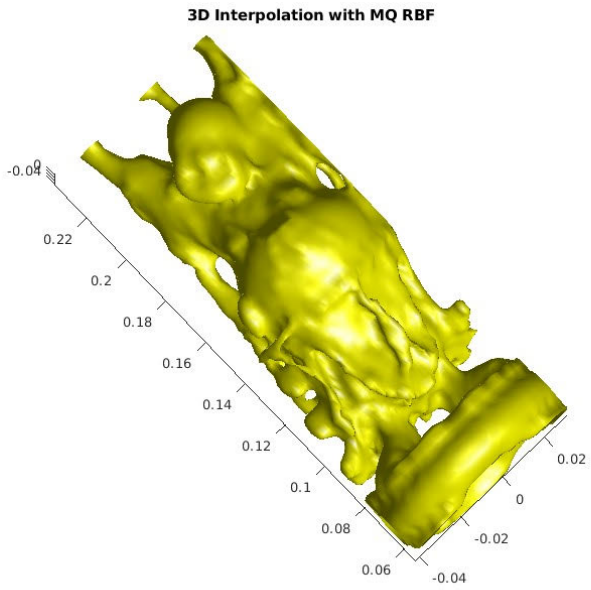

Figure 6: Buddha Surface Reconstruction with 60 Evaluation Points using the $\mathbf{coe} = \text{pinv}(\mathbf{IM}) \times \mathbf{rhs}$ Method, with a Large Dataset of around 18,000 Points. Despite the ample dataset size, the reconstruction quality using the $\mathbf{coe} = \text{pinv}(\mathbf{IM}) \times \mathbf{rhs}$ method falls short when compared to the $\mathbf{coe} = \mathbf{IM}/\mathbf{rhs}$ method, even in scenarios with smaller datasets. The latter method demonstrates superior performance, producing high-quality reconstructions even with limited data points. This observation underscores the impact of the coefficient computation method on the reconstruction outcome, emphasizing the efficacy of $\mathbf{coe} = \mathbf{IM}/\mathbf{rhs}$ for achieving superior surface reconstructions.

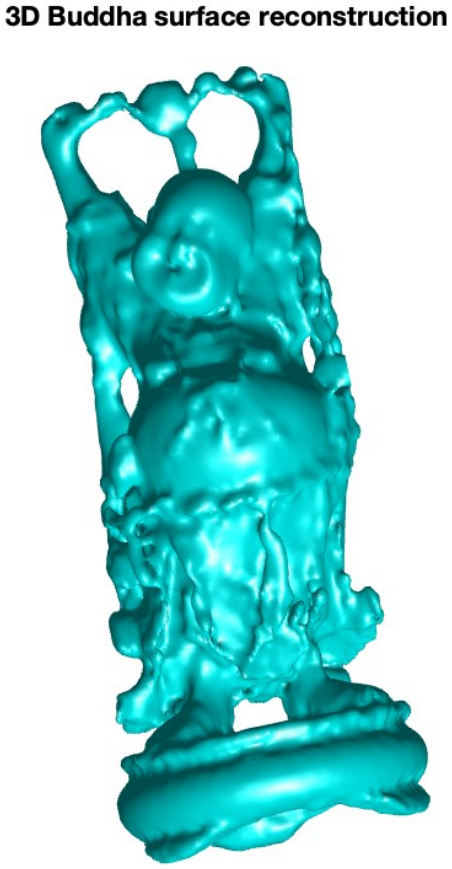

Figure 7: Buddha Surface Reconstruction with 150 Evaluation Points using 11,200 Data Points and the **coe** = **IM**/**rhs** Method. The surface reconstruction showcases exceptional quality, leveraging the **coe** = **IM**/**rhs** method with a dataset of 11,200 points. This methodology excels in capturing intricate details, resulting in a high-fidelity representation of the Buddha's form. The superior quality of the reconstruction emphasizes the effectiveness of the **coe** = **IM**/**rhs** approach for achieving optimal results in surface reconstruction endeavors .

Figure 8: Surface Reconstruction of the Buddha with 350 Evaluation Points and 18,000 Data Points using the $\mathbf{coe} = \text{pinv}(\mathbf{IM}) \times \mathbf{rhs}$ Method. Despite employing a substantial dataset of 18,000 points and utilizing the $\mathbf{coe} = \text{pinv}(\mathbf{IM}) \times \mathbf{rhs}$ method for coefficient computation, the resulting surface reconstruction at 350 evaluation points reveals limitations in achieving a high-quality representation. The intricate details of the Buddha's form are not adequately captured, and the reconstructed surface exhibits noticeable deviations from the expected structure. This observation underscores the challenges associated with the $\mathbf{coe} = \text{pinv}(\mathbf{IM}) \times \mathbf{rhs}$ method for optimal surface reconstruction in this specific scenario. Further investigations and considerations may be necessary to enhance the fidelity of the reconstructed surface and explore alternative methodologies for improved results.

and more refined representation. This observation aligns with the principle that a higher density of data facilitates a more accurate rendering of complex geometries. Thus, the findings in figure 6 highlight the progressive improvement in surface reconstruction as the dataset's granularity is augmented, emphasizing the pivotal role of data quantity in achieving enhanced visual fidelity.

Our experimentation involved systematically altering the number of points, with a particular focus on higher *neval* values. The results unequivocally demonstrated that a higher *neval* value led to superior surface quality compared to scenarios with lower *neval* values, as visually evident in the figures. It is noteworthy that despite the computational demands associated with a *neval* value of 150, the benefits in terms of surface smoothness were substantial. The computational time of approximately 3 minutes for this configuration attests to the feasibility of implementing such a strategy even with a large dataset. The utilization of Delaunay triangulation for normal points selection played a crucial role in our approach. This method ensured the systematic and efficient identification of normal points, contributing to the consistency of our results across various *neval* values.

In summary, our findings underscore the importance of carefully selecting the *neval* parameter in surface reconstruction processes. The trade-off between computational time and surface quality is evident, and our study suggests that a *neval* value of 150 strikes a favorable balance, yielding a remarkably smooth surface reconstruction. This research not only enhances our understanding of the nuances in surface reconstruction but also provides a practical guideline for optimizing *neval* parameters in similar applications.